

How surface-specific is 2nd-order non-linear spectroscopy? ^{EP}

Cite as: J. Chem. Phys. **151**, 230901 (2019); <https://doi.org/10.1063/1.5129108>

Submitted: 26 September 2019 . Accepted: 20 November 2019 . Published Online: 16 December 2019

Shumei Sun, Jan Schaefer, Ellen H. G. Backus ^{id}, and Mischa Bonn ^{id}

COLLECTIONS

^{EP} This paper was selected as an Editor's Pick



View Online



Export Citation



CrossMark

ARTICLES YOU MAY BE INTERESTED IN

[Unveiling coupled electronic and vibrational motions of chromophores in condensed phases](#)

The Journal of Chemical Physics **151**, 200901 (2019); <https://doi.org/10.1063/1.5128388>

[Polymer physics across scales: Modeling the multiscale behavior of functional soft materials and biological systems](#)

The Journal of Chemical Physics **151**, 230902 (2019); <https://doi.org/10.1063/1.5126852>

[Adventures in DFT by a wavefunction theorist](#)

The Journal of Chemical Physics **151**, 160901 (2019); <https://doi.org/10.1063/1.5116338>





Lock-in Amplifiers

Zurich
Instruments

Watch the Video



How surface-specific is 2nd-order non-linear spectroscopy?

Cite as: J. Chem. Phys. 151, 230901 (2019); doi: 10.1063/1.5129108

Submitted: 26 September 2019 • Accepted: 20 November 2019 •

Published Online: 16 December 2019



Shumei Sun,^{1,2,a)} Jan Schaefer,^{1,a)} Ellen H. G. Backus,^{1,2,b)}  and Mischa Bonn^{1,b)} 

AFFILIATIONS

¹Max Planck Institute for Polymer Research, Ackermannweg 10, 55128 Mainz, Germany

²Department of Physical Chemistry, University of Vienna, Währinger Strasse 42, 1090 Vienna, Austria

^{a)}**Contributions:** S. Sun and J. Schaefer contributed equally to this work.

^{b)}**Authors to whom correspondence should be addressed:** backus@mpip-mainz.mpg.de and bonn@mpip-mainz.mpg.de

ABSTRACT

Surfaces and interfaces play important roles in many processes and reactions and are therefore intensively studied, often with the aim of obtaining molecular-level information from just the interfacial layer. Generally, only the first few molecular layers next to the interface are relevant for the surface processes. In the past decades, 2nd-order nonlinear spectroscopies including sum-frequency generation and second harmonic generation have developed into powerful tools for obtaining molecularly specific insights into the interfacial region. These approaches have contributed substantially to our understanding of a wide range of physical phenomena. However, along with their wide-ranging applications, it has been realized that the implied surface-specificity of these approaches may not always be warranted. Specifically, the bulk quadrupole contribution beyond the electric dipole-approximation for a system with a weak nonlinear interface signal, as well as the diffuse layer contribution at charged interfaces, could mask the surface information. In this perspective paper, we discuss the surface-specificity of 2nd-order nonlinear spectroscopy, especially considering these two contributions.

Published under license by AIP Publishing. <https://doi.org/10.1063/1.5129108>

I. INTRODUCTION

Interfacial phenomena are relevant for many atmospheric, geochemical, and electrocatalytic processes. Molecular-level insight into such interfaces is important not only for a basic understanding of interfacial processes and their effect on macroscopic scales but also for engineering, for example, new catalyst surfaces. Spectroscopy provides a direct and potentially chemically selective probe of molecular properties. In particular, vibrational spectroscopy techniques are extensively used not only because of their chemical selectivity but also for their potential to report on the structure and dynamics of molecules within their chemical environment. For studying interfaces, various spectroscopic techniques have been adapted to suppress the bulk response and only retrieve the interfacial information. Besides Attenuated Total Reflection (ATR), tip- or surface-enhanced Raman spectroscopy (TERS/SERS), and Electron Spin Resonance (ESR), 2nd-order nonlinear techniques are increasingly used to study interfacial systems. ATR, a well-established technique since the early 1960s, provides interfacial sensitivity on the micrometer range that is limited by the length scale of the

evanescent wave of the reflected light. For molecules preferentially oriented at an interface, IR-based polarization modulation techniques have also been applied.¹ Plasmon-enhanced Raman and nonlinear techniques may reach up to nanometer spatial resolution and are complementary in terms of their applicability. Enhanced Raman spectroscopies require the presence of a metal in the form of a coated surface, nanoparticles, or tip, and the surface sensitivity is limited by the field associated with plasmonic resonances of the corresponding metals. This is beneficial for studying topological and electrochemical properties of surface nanostructures down to length scales of single molecules as relevant for engineering new electrode materials.^{2–5} ESR relies on the presence of a probe molecule containing an unpaired electron; the use of probe molecules always raises the question as to what extent these affect the interfacial molecular structure.

2nd-order nonlinear techniques such as sum-frequency generation (SFG) and second harmonic generation (SHG) provide an intrinsic surface selectivity under the electric dipole (ED) approximation for a centrosymmetric medium and have been widely used for studying surfaces and interfaces.^{6–8} Under the ED

approximation, 2nd-order nonlinear processes are only allowed for the region where the symmetry is broken, which is, per definition, the case at the interface due to its anisotropic environment. Conversely, 2nd-order nonlinear processes are symmetry-forbidden in bulk. As a consequence, SFG/SHG is generated only at the interfaces and molecular information of the interface can be obtained. However, the interfacial sensitivity of 2nd-order nonlinear techniques depends on the physical properties of the investigated system. In the development of SFG/SHG, it has been recognized that there are two main effects that may limit the surface specificity of the approaches: (1) Beyond the electric dipole approximation, higher-order terms such as quadrupoles may give rise to contributions to the nonlinear response.^{6,9–12} Since contributions from electric quadrupole transitions are not constrained by the above-mentioned symmetry selection rule, these can contribute to the overall 2nd-order signal from a centrosymmetric bulk medium. Depending on the relative magnitudes of dipole and quadrupole contributions, the surface information could be washed out by the overwhelming bulk response. (2) For charged interfaces, the intrinsic symmetry breaking at the interface can exceed the typical 1–2 monolayers as found for neutral interfaces.^{13–16} This is related to the formation of the so-called electric double layer (EDL) at charged interfaces, associated with the long-ranging surface potential. Interactions with this electric field may also cause reorientation and/or polarization of water molecules not directly at, but in the proximity of, the surface, which both give rise to symmetry-breaking that allows a 2nd-order nonlinear response. As a consequence, the probing depth may vary, depending on the interfacial charge distribution, which determines the thickness of the EDL. In this work, we will discuss how the surface specificity of 2nd-order nonlinear spectroscopy is affected by each of those two aspects.

II. QUADRUPOLE CONTRIBUTION

When interacting with matter, a plane electromagnetic wave does so not only through its electric and magnetic field components but also through the space- and time-derivatives of these fields.¹⁷ For example, the electric field of a wave is not uniform along the path through an object, due to its finite wavelength. Thus, for the light-matter interaction, not just the fields but also the associated field gradients and their time derivatives may play a role. From perturbation theory, up to the first derivatives of the fields, the effective 2nd-order polarization can be expressed as¹⁰

$$\mathbf{P}_{\text{eff}}^{(2)}(z) = \chi_d^{(2)}(z) : \mathbf{E}_{\omega 1} \mathbf{E}_{\omega 2} + \chi_{q,\omega 1}^{(2)}(z) : \nabla \mathbf{E}_{\omega 1} \mathbf{E}_{\omega 2} + \chi_{q,\omega 2}^{(2)}(z) : \mathbf{E}_{\omega 1} \nabla \mathbf{E}_{\omega 2} - \nabla \cdot (\chi_{q,\omega 3}^{(2)}(z) : \mathbf{E}_{\omega 1} \mathbf{E}_{\omega 2}), \quad (1)$$

where the last three terms represent the quadrupole contribution, $\chi_{q,\omega i}^{(2)}$, which includes both the electric quadrupole and magnetic dipole parts.¹⁸ Under the ED approximation, only the first term of Eq. (1) is considered, and the last three quadrupole terms are neglected. This is often valid, considering that, at any given moment in time, the typical length scale over which the field amplitude (λ) varies is large compared with typical molecular dimensions (a). One can show that $\chi_q^{(2)} \sim \chi_d^{(2)} \cdot a$ and the interaction of the quadrupole and the field gradient can be roughly approximated by $\chi_q^{(2)} k$ (with

$k \propto 1/\lambda$ being the wave-vector of the electromagnetic wave) so that $\chi_q^{(2)} k \sim \chi_d^{(2)} \frac{a}{\lambda} \ll \chi_d^{(2)}$.^{19,20} On the other hand, quadrupole contributions may become significant in the case of a dramatic change of the electric field amplitude across the interface and due to the large volume over which the induced quadrupole moment is integrated. Indeed, the quadrupole in bulk contributes to SFG/SHG over the coherence length (typically ranging from tens of nanometers to micrometers), which is usually much larger than the typical subnanometer thickness of the interface. Moreover, for centrosymmetric molecules with a negligible dipole, such as benzene, the 2nd-order nonlinear response may be dominated by quadrupole terms. Thus, for a centrosymmetric medium, without any prior knowledge of the investigated system, the assumption that SFG/SHG signal originates from the near-top-monolayer is not necessarily valid.^{9,10,21}

For identifying the surface-specificity of nonlinear spectroscopy, it is fundamentally important to evaluate the bulk and surface contributions to the overall response. The challenge is that there is no simple theory that can be used to disentangle those components properly. To determine the physical origin of the nonlinear response and quantitatively evaluate surface and bulk contributions, a comprehensive theory of dipole and quadrupole contributions and the formalism of the effective 2nd-order nonlinear susceptibility are needed.

In the past 50 years, there has been much theoretical work on dipole and quadrupole contributions, leading to a unified unambiguous formalism of the effective susceptibility.^{6,12,22} Let us consider a surface system as shown in Fig. 1; the interface thickness is $d = 0^+ - 0^-$. For $z < 0^-$, the material properties are bulklike. Considering the dipole and quadrupole contributions, the effective nonlinear susceptibility is given by

$$\chi_{\text{eff}}^{(2)} = \chi_D^{(2)} + \chi_{IQ}^{(2)} + \chi_{q,\omega 3}^{(2)} + \frac{\chi_{BB}^{(2)}}{i\Delta k_z}, \quad (2)$$

where $\Delta k_z = k_{\omega 1,z} + k_{\omega 2,z} - k_{\omega 3,z}$ is the mismatch of the wavevectors along the surface normal in the bulk. More details of the derivation can be found in textbooks.^{6,23} $\chi_{\text{eff}}^{(2)}$ is obtained by integrating $\mathbf{P}_{\text{eff}}^{(2)}(z)$ in Eq. (1) over the region from $-\infty$ to 0^+ . The first term ($\chi_D^{(2)}$) stems

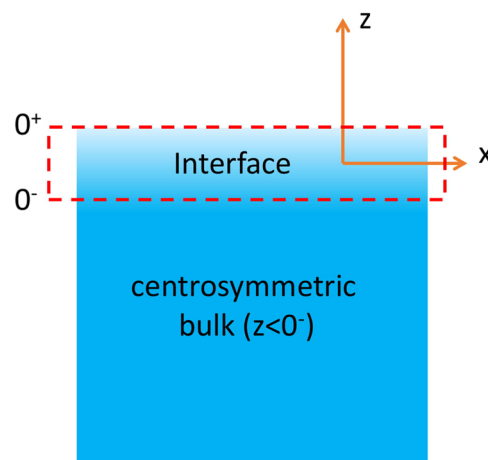


FIG. 1. Schematic of the liquid/air interface, with the interface defined as the region between $z = 0^-$ and $z = 0^+$.

from the integration of $\chi_d^{(2)}(z)$ only over the interface region, as $\chi_d^{(2)}(z)$ vanishes in the bulk. One should note that the spatial derivative of the electric field contains two parts: one is the dramatic amplitude change across the interface and the other is more slowly varying due to the change in the phase along the propagation in the bulk. Correspondingly, one can distinguish an interfacial quadrupole term $\chi_{IQ}^{(2)}$ and a “true” bulk term $\frac{\chi_{BB}^{(2)}}{i\Delta k_z}$, associated, respectively, with the integration of the electric field gradient over the interface and over the bulk. $\chi_{q,\omega_3}^{(2)}$ originates from the integration by parts of the last term in Eq. (1). As $\chi_{q,\omega_3}^{(2)}(z)$ is discontinuous across the interface, the integration of the derivative of $\chi_{q,\omega_3}^{(2)}(z)$ can be simply treated as the difference between $\chi_{q,\omega_3}^{(2)}$ of the upper and lower media. Here, the nonlinear susceptibility of the upper medium is assumed to be zero; thus, $\chi_{q,\omega_3}^{(2)}$ entirely reflects the properties of the bulk and contains no information about the surface.

Equation (2) shows that the effective 2nd-order nonlinear susceptibility consists of four distinct physical components. From an experimental point of view, one can readily separate the last term, $\frac{\chi_{BB}^{(2)}}{i\Delta k_z}$, from the first three components because its contribution is beam geometry-dependent. The contribution of $\frac{\chi_{BB}^{(2)}}{i\Delta k_z}$ has been discussed in previous works, where it was demonstrated to be negligible in reflection SFG configuration.^{20,21,24} However, in the transmitted configuration, the SFG signal can be dominated by $\frac{\chi_{BB}^{(2)}}{i\Delta k_z}$ as the coherence length Δk_z^{-1} in transmission is much larger than in the reflected configuration. The other two quadrupole terms $\chi_{IQ}^{(2)}$ and $\chi_{q,\omega_3}^{(2)}$ always appear together with the surface dipole contribution, and thus, they are called inseparable terms. Therefore, it is essential to evaluate the contribution of $\chi_{IQ}^{(2)}$ and $\chi_{q,\omega_3}^{(2)}$ to $\chi_{eff}^{(2)}$ explicitly before one can deduce if the SFG/SHG spectrum reports on the surface structure. Tahara and co-workers have studied the potential quadrupole contribution to the nonresonant SFG signal by measuring eight different liquid surfaces, including water, through heterodyne measurements with different polarization combinations, with the incoming lights being off-resonant with molecular transitions.²⁵ They concluded that quadrupole terms ($\chi_{IQ}^{(2)}$ and $\chi_{q,\omega_3}^{(2)}$) dominate the nonresonant SFG signal, and the sign of the imaginary spectrum has no relation to the up vs down alignment of interfacial molecules. Computational analyses of the water/air interface have confirmed the above conclusion. For ssp and sps polarization combinations, the simulation shows that the $\chi_{q,\omega_3}^{(2)}$ -term is roughly 4 times larger than $\chi_D^{(2)}$ for the nonresonant SFG/SHG signal.²⁶

Especially, for a centrosymmetric molecule, the quadrupole contribution at resonance could dominate the SFG signal as the dipole response is inherently suppressed. As such, the air/benzene interface has been studied with 2nd-order nonlinear optical methods by several groups.^{24,27–30} Tahara and co-workers have studied this system using different polarization combinations and assigned all the resonances to the quadrupole contribution,^{29,30} which is inconsistent with simulation results predicting both dipole and quadrupole contributions.²⁸ Tian and co-workers performed another set of experimental measurements. Using heterodyne SFG

measurements in reflection and special transmission beam geometries to determine the contribution of $\chi_{q,\omega_3}^{(2)}$ independently, they verified that quadrupole contributions cannot be neglected.²⁴ In particular, the quadrupole contribution is dominant in sps polarization combination, while in ssp polarization, their data shows that both dipole and quadrupole contribute to the measured SFG signal.²⁴ The method used by Tian offers a general guideline to quantitatively evaluate the quadrupole contribution for a nonpolar medium. To further resolve the debate on the physical origin of the SF response of benzene, direct measurements of the imaginary part of the response of benzene on modified surfaces is needed, e.g., silica/benzene and silica/OTS/benzene interfaces. In case the quadrupole contribution is dominant, the spectra should be very similar for the different surfaces. However, if the dipole term also plays a role, the spectral shape is expected to be different.

The most important and the most investigated systems by SFG/SHG are water interfaces. Unfortunately, there is no feasible experimental method to quantitatively separate its quadrupole contribution from the effective SFG/SHG spectrum. Generally, it is assumed that the surface dipole contribution is dominant in the ssp polarization combination for the O–H stretching resonance. Many experiments employing differently modified surfaces support this notion. Moreover, simulation results can well reproduce the SFG spectrum of the air/water interface without taking any quadrupole contribution into account.^{31–33} Although the O–H stretch resonance is typically surface dipole-dominated, substantial controversy exists in interpreting the signal from the H–O–H bending mode of water. Tahara and co-workers have concluded that the SFG signal of the bending mode is dominated by the quadrupole contribution with the calculation results of $\text{Im } \chi_D^{(2)} : \text{Im } \chi_{q,\omega_3}^{(2)} \sim 1 : 8.7$,³⁴ while more recent experimental results can be rationalized by the assumption that the SFG signal of the bending mode originates primarily from the dipole contribution.^{35–37} In addition, simulation results have indicated that the surface dipole contribution is not weak.^{37–39} Recently, a study by Nagata and co-workers showed that the dipole contribution dominates $\chi^{(2)}$ for the bending mode both for the air/water interface and the charged lipid/water interface.⁴⁰ To resolve the discrepancy between different experimental results in the bending mode region, further efforts are surely needed.

Generally, the 2nd-order nonlinear spectroscopy in reflection geometry is a surface-specific technique for most surfaces with a polar-oriented layer. For nonpolar media, one can follow the guideline provided in Ref. 24 to separate surface and bulk contributions. As no experimental method is capable of quantitatively separating surface and bulk contributions, to be certain whether SFG/SHG is surface specific for certain interfacial systems, one might have to perform additional measurements such as modifying the surface or to rely on independent MD simulations.¹⁹ Overall, care must be taken by studying unknown systems without any prior knowledge, especially for those with a weak 2nd-order nonlinear response.

III. LIQUIDS AT CHARGED SURFACES

Many surfaces in contact with liquids, and specifically water, are known to be charged, including biological membranes, electrochemical electrodes, and mineral surfaces. The presence of charge

gives rise to physical phenomena such as the surface potential. As a consequence of the surface charge, the composition and the structure of the aqueous solution in close proximity to the surface differ from that of bulk water. This interfacial region is referred to as the Electric Double Layer (EDL). Several models exist to describe the EDL,^{41–45} with the Gouy-Chapman-Stern model being the commonly used, which is schematically presented in Fig. 2 for the negatively charged silica surface in contact with water.

The nature of the EDL not only determines the physical properties of the surface but also controls its reactivity. Therefore, microscopic insights are required to get a fundamental understanding of the microscopic and molecular physical and chemical phenomena that also determine the behavior on macroscopic scales. The advantage of employing nonlinear spectroscopy compared to traditional methods such as the potentiometric titration is its ability to access molecular-level information of the EDL. Based on the traditional picture (the Gouy-Chapman model), the following discussion elaborates on the molecular composition of EDLs, the resulting physical properties, and how they are reflected by nonlinear spectroscopy.

For the example of silica (Fig. 2), its charge results from the deprotonation of silanol groups (O–H groups terminating the SiO₂

lattice) upon contact with water. The water molecules interacting with the surface charges or their associated electric field E_0 differ from bulk water and represent the EDL. The decay of the corresponding surface potential $[\phi(z)]$ reports on two regions of the EDL, namely, the near-surface region, in which the potential drops linearly, similar to what is known for parallel plate capacitors, and the more distant region that shows a more gradual decay of the potential [Fig. 2(b)]. The near-surface part is often referred to as the Stern layer (SL)⁴⁶ or also the Bonded Interfacial Layer (BIL),⁴⁷ depending on the definition. The outer region is called the Diffuse Layer (DL).

Symmetry breaking that gives rise to a finite nonlinear optical response from the charged interface region can occur for two reasons: first of all, in the region close to the surface where the molecules experiencing an anisotropic environment, the symmetry is naturally broken. Second, the electrostatic field induced by the surface charge can reorient or polarize water molecules in the region of EDL and thus lifts the centrosymmetry.^{15,48} Both effects give rise to an effective breaking of the centrosymmetry which is required for the 2nd-order nonlinear activity. For the second mechanism, the decay of the surface electric field, i.e., the thickness of the EDL, determines the SFG/SHG probing depth and intensity for a charged interface. To take the potentially long-ranging surface electric field E_0 into account, the description of 2nd-order nonlinear spectroscopy has to be extended: an additional 3rd-order term has been invoked to describe the decay of E_0 away from the surface.^{46,47,49–54}

The pioneering work in this field has been presented by Eisenthal and co-workers,⁴⁹ in which they deduced surface potentials (ϕ_0) of the silica/water interface from SHG intensities at different bulk pH conditions. For this purpose, they expressed the 2nd-order nonlinear response ($I_{\omega 3} \propto |E_{\omega 3}|^2$) of a charged surface as a sum of a 2nd-(surface close) term and a 3rd-order (distant) term,

$$E_{\omega 3} \propto P_{\omega 3} = \chi^{(2)} E_{\omega 1} E_{\omega 2} + \int_{-\infty}^0 \chi^{(3)} E_0 E_{\omega 1} E_{\omega 2} dz. \quad (3)$$

In this expression, the integrated term can be written as $-\chi^{(3)} \phi_0 E_{\omega 1} E_{\omega 2}$ by assuming an isotropic field being zero far away from the surface,

$$-\phi_0 = \int_{-\infty}^0 E_0(z) dz = \int_{-\infty}^0 \left(-\frac{d}{dz} \phi(z) \right) dz. \quad (4)$$

In this framework, the neat interfacial response $\chi^{(2)}$ results from the near-surface water layers which are reoriented by the surface charges, accounting for the SL. An additional third-order term $\chi^{(3)}$ accounts for the more outer water layers (DL) that are orientated and/or polarized due to the interaction with the longer-ranged charge-induced surface-electric field E_0 .

Hore and co-workers have previously presented an experimental effort to disentangle those two contributions to the SFG response of water in front of a silica surface. In their experiments, they made use of the fact that the surface field can be effectively screened by ions in the solution. By varying the ionic strength and thereby tuning the decay length of E_0 , they were able to deduce the relative $\chi^{(2)}$ and $\chi^{(3)}$ contributions to the total SFG signal.⁵² A breakthrough in the separation of the $\chi^{(2)}$ and $\chi^{(3)}$ contributions for a charged surface was made by Tian and co-workers. They were the first to experimentally

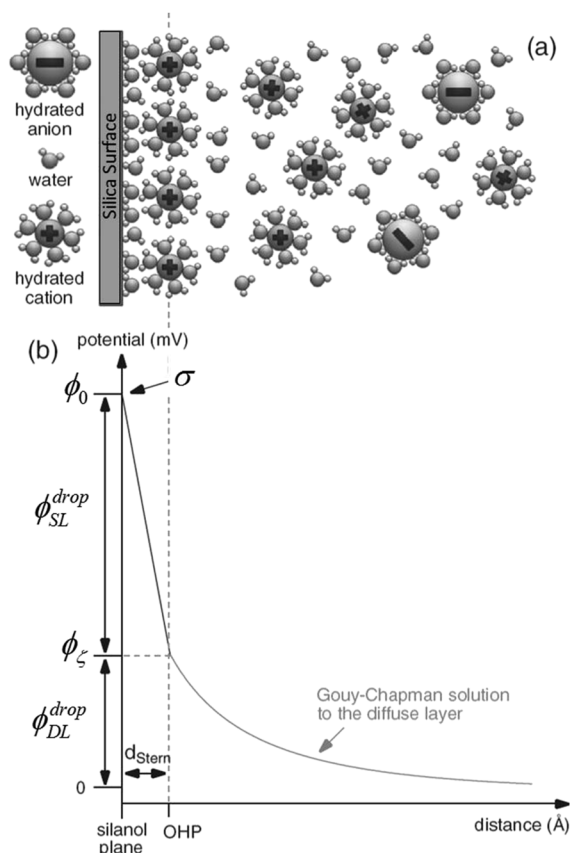


FIG. 2. (a) Ion and water distribution of an aqueous electrolyte in front of a negatively charged silica surface. (b) The associated surface potential decay predicted by the Gouy-Chapman-Stern model of the electric double layer for such a system. Figures are adapted from Ref. 45.

obtain the $\chi^{(3)}$ spectrum of water by heterodyne sum-frequency generation measurements by considering the modulation of the Debye length and the coherence length in the sum-frequency spectra analysis for a charged surface. With increasing probing depth, the generated SFG light is increasingly poorly phase-matched, which affects the shape and intensity of the resulting spectrum.⁴⁷ Mathematically, this phase mismatch for SFG photons generated at different probing depths (z) is accounted for by considering the difference between the z -components of the corresponding wave vectors, Δk_z .

Using the above scheme, Gonella *et al.* discussed the second-order nonlinear response of an aqueous solution with varying ionic strength in front of a charged surface.⁴⁶ In the model, the approximate solution of the Debye-Hückel theory is used to describe the decay of the electric potential that is associated with the electric field E_0 ,

$$\phi(z) = \phi_0 e^{\kappa z} \quad (z \leq 0) \quad (5)$$

with κ^{-1} being the ionic-strength-dependent Debye length. As a consequence, κ^{-1} can be used to relate the ionic strength to the resulting SFG/SHG probing depth. In combination with the z -dependent phase mismatch introduced above, their proposed model predicts the variation of the nonlinear response as a function of ionic strength,

$$\begin{aligned} I_{\omega 3} &\propto \left| \chi^{(2)} + \chi^{(3)} \int_{-\infty}^0 \left(-\frac{d}{dz} \phi(z) \right) e^{i\Delta k_z z} dz \right|^2 \\ &= \left| \chi^{(2)} - \chi^{(3)} \phi_0 \frac{\kappa}{\kappa + i\Delta k_z} \right|^2. \end{aligned} \quad (6)$$

The result is presented schematically in Fig. 3(a), showing the total SFG/SHG intensity ($I_{\omega 3}$, red) along with the underlying variation of the screening effect ($|\chi^{(2)} - \chi^{(3)} \phi_0|^2$, green) and the optical interference term ($|\frac{\kappa}{\kappa + i\Delta k_z}|$, blue). The associated Debye screening lengths are presented on the upper axis. It predicts that at a given surface charge, the nonlinear response increases with increasing screening length, i.e., decreasing ionic strength. However, at very low (submillimolar) ionic strengths, the overall signal decreases again due to increasing destructive interference of the emitted SFG/SHG light for Debye lengths exceeding 10s of nanometers. Experimental evidence for the applicability of this model has been presented, among others, in detail in Refs. 55 and 56. Figure 3(b) shows the experimental SHG/SFG results on the fused silica/water interface with varying NaCl concentrations. The increasing-decreasing trend is in good agreement with the theoretical prediction. The signal enhancement factor at the ion concentration of 10^{-4} – 10^{-3} M is different between the SHG and SFG intensities, which is likely due to the different values of the ratio, $\chi^{(3)}/\chi^{(2)}$, for the nonresonant and resonant contributions, at the silica/water interface.

In total, interfacial layer sensitivity is reached not only at high ion concentration (~ 1 M), where the Debye length is very short and the surface charge is sufficiently screened, but also for very dilute solutions ($< \text{micromolar}$), where the Debye length is on the order of, or larger than, the wavelength of the SFG light, and as a result, destructive interference from the different regions across the diffuse layer can occur. In the intermediate concentration regime ($\sim \text{millimolar}$), the diffuse layer contribution to the total response is

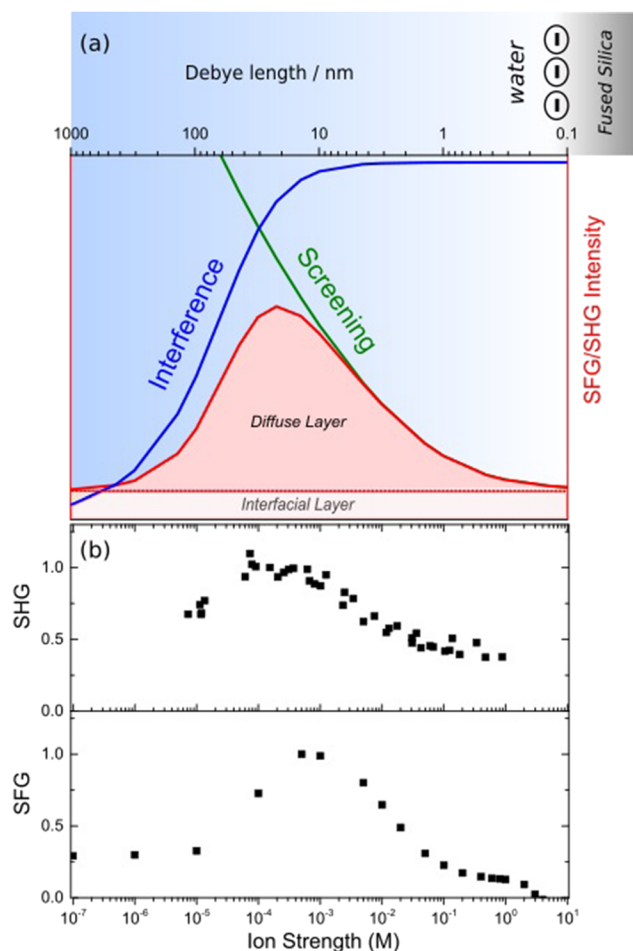


FIG. 3. (a) Theoretical SFG/SHG response of a charged mineral surface in contact with varying ion concentration.^{46,47} (a) is adapted from Ref. 55. (b) Experimental SHG⁵⁶ and SFG⁵⁵ results obtained at the silica/water interface with varying bulk NaCl concentrations.

the largest, where the Debye length is comparable with the coherence length in reflection corresponding to 10s of nanometers. A rough estimation of the $\chi^{(3)}$ contribution in experiments employing ssp polarization combination results in $|\text{Im}\chi^{(2)}| \sim 1 \times 10^{-21} \text{ m}^2/\text{V}$ (pure water)^{57,58} and $|\text{Im}\chi^{(3)}| \sim 4 \times 10^{-20} \text{ m}^2/\text{V}^2$.⁴⁷ For $\phi_0 \sim 0.02 \text{ V}$, the $|\text{Im}\chi^{(3)} \phi_0|$ contribution to the SFG signal is comparable to that of the surface contribution $|\text{Im}\chi^{(2)}|$. A simulation study is consistent with estimations based on experimental results.¹⁵

IV. CONCLUSION

2nd-order nonlinear spectroscopies have been widely applied in surface or interface studies. However, their surface specificity is not always clear. In this paper, we discussed the surface specificity of 2nd-order nonlinear spectroscopy from two aspects that might mask the surface information: quadrupole contribution and $\chi^{(3)}$

contribution. For a system with a weak SFG signal, bulk quadrupole contributions can dominate; for a charged interface, the contribution from the diffuse layer cannot be neglected except in the limits of very low (<micromolar) and very high (>1M) electrolyte concentrations. Therefore, care must be taken to interpret SFG/SHG spectra as reflecting the surface properties since the technique is not always surface specific. While previous experimental approaches (e.g., comparing reflected to transmitted SFG signals²⁴) have shed some light on disentangling bulk and surface contributions, this remains challenging. One way forward may be to utilize heterodyne measurements because, in the imaginary spectrum, each (i.e., bulk and surface) contribution is simply the sum of the individual contributions, simplifying the spectral analysis. However, even with additive contributions to the overall signals, excluding or evaluating the bulk contributions will remain challenging in many cases from only experimental SFG results since the bulk and surface responses are generally quite similar in their spectral shape. It, therefore, seems that only clever experiments combined with high-quality simulations (including spectral response calculations) will be able to quantify surface and bulk contributions and to obtain the real surface information using nonlinear spectroscopy. Currently, quantitative discrepancies remain between the experiment and simulation for several interfacial systems. With improved accuracy and dependability of both experiments and simulations, and their productive interplay, disentangling the different contributions to surface spectroscopic signals will become increasingly straightforward.

ACKNOWLEDGMENTS

The authors thank Franz Geiger for sharing his results with us. This work was funded by an ERC Starting Grant (Grant No. 336679) and the MaxWater initiative of the Max Planck Society.

REFERENCES

- 1 E. A. Monyoncho, V. Zamlynny, T. K. Woo, and E. A. Baranova, *Analyst* **143**(11), 2563–2573 (2018).
- 2 Z.-Q. Tian, B. Ren, J.-F. Li, and Z.-L. Yang, *Chem. Commun.* **2007**(34), 3514–3534.
- 3 J. F. Li, Y. F. Huang, Y. Ding, Z. L. Yang, S. B. Li, X. S. Zhou, F. R. Fan, W. Zhang, Z. Y. Zhou, and B. Ren, *Nature* **464**(7287), 392 (2010).
- 4 A. B. Zrimsek, N. Chiang, M. Mattei, S. Zaleski, M. O. McAnally, C. T. Chapman, A.-I. Henry, G. C. Schatz, and R. P. Van Duyne, *Chem. Rev.* **117**(11), 7583–7613 (2016).
- 5 S.-Y. Ding, J. Yi, J.-F. Li, B. Ren, D.-Y. Wu, R. Panneerselvam, and Z.-Q. Tian, *Nat. Rev. Mater.* **1**(6), 16021 (2016).
- 6 Y. Shen, *Fundamentals of Sum-Frequency Spectroscopy* (Cambridge University Press, 2016).
- 7 G. Richmond, *Chem. Rev.* **102**(8), 2693–2724 (2002).
- 8 Z. Chen, *Prog. Polym. Sci.* **35**(11), 1376–1402 (2010).
- 9 N. Bloembergen, R. K. Chang, S. Jha, and C. Lee, *Phys. Rev.* **174**(3), 813 (1968).
- 10 P. Guyot-Sionnest and Y. Shen, *Phys. Rev. B* **38**(12), 7985 (1988).
- 11 B. Koopmans, A. Janner, H. Wierenga, T. Rasing, G. Sawatzky, and F. van der Woude, *Appl. Phys. A* **60**(2), 103–111 (1995).
- 12 K. Shiratori and A. Morita, *Bull. Chem. Soc. Jpn.* **85**(10), 1061–1076 (2012).
- 13 A. Morita and J. T. Hynes, *Chem. Phys.* **258**(2–3), 371–390 (2000).
- 14 A. Morita and J. T. Hynes, *J. Chem. Phys. B* **106**(3), 673–685 (2002).
- 15 T. Joutsuka, T. Hirano, M. Sprik, and A. Morita, *Phys. Chem. Chem. Phys.* **20**(5), 3040–3053 (2018).
- 16 S. Pezzotti, D. R. Galimberti, Y. R. Shen, and M.-P. Gaigeot, *Phys. Chem. Chem. Phys.* **20**(7), 5190–5199 (2018).
- 17 R. E. Raab, O. L. De Lange, and O. L. de Lange, *Multipole Theory in Electromagnetism: Classical, Quantum, and Symmetry Aspects, with Applications* (Oxford University Press, 2005), On Demand.
- 18 S. J. Byrnes, P. L. Geissler, and Y. Shen, *Chem. Phys. Lett.* **516**(4–6), 115–124 (2011).
- 19 Y. Shen, *Appl. Phys. B* **68**(3), 295–300 (1999).
- 20 H. Held, A. Lvovsky, X. Wei, and Y. Shen, *Phys. Rev. B* **66**(20), 205110 (2002).
- 21 X. Wei, S.-C. Hong, A. Lvovsky, H. Held, and Y. R. Shen, *J. Chem. Phys. B* **104**(14), 3349–3354 (2000).
- 22 Y. Shen, *J. Phys. Chem. C* **116**(29), 15505–15509 (2012).
- 23 A. Morita, *Theory of Sum Frequency Generation Spectroscopy* (Springer, 2018).
- 24 S. Sun, C. Tian, and Y. R. Shen, *Proc. Natl. Acad. Sci. U. S. A.* **112**(19), 5883–5887 (2015).
- 25 S. Yamaguchi, K. Shiratori, A. Morita, and T. Tahara, *J. Chem. Phys.* **134**(18), 184705 (2011).
- 26 K. Shiratori, S. Yamaguchi, T. Tahara, and A. Morita, *J. Chem. Phys.* **138**(6), 064704 (2013).
- 27 E. L. Hommel and H. C. Allen, *Analyst* **128**(6), 750–755 (2003).
- 28 T. Kawaguchi, K. Shiratori, Y. Henmi, T. Ishiyama, and A. Morita, *J. Phys. Chem. C* **116**(24), 13169–13182 (2012).
- 29 K. Matsuzaki, S. Nihonyanagi, S. Yamaguchi, T. Nagata, and T. Tahara, *J. Phys. Chem. Lett.* **4**(10), 1654–1658 (2013).
- 30 K. Matsuzaki, S. Nihonyanagi, S. Yamaguchi, T. Nagata, and T. Tahara, *J. Chem. Phys.* **151**(6), 064701 (2019).
- 31 G. R. Medders and F. Paesani, *J. Am. Chem. Soc.* **138**(11), 3912–3919 (2016).
- 32 T. Ohto, K. Usui, T. Hasegawa, M. Bonn, and Y. Nagata, *J. Chem. Phys.* **143**(12), 124702 (2015).
- 33 Y. Ni and J. Skinner, *J. Chem. Phys.* **145**, 031103 (2016).
- 34 A. Kundu, S. Tanaka, T. Ishiyama, M. Ahmed, K.-i. Inoue, S. Nihonyanagi, H. Sawai, S. Yamaguchi, A. Morita, and T. Tahara, *J. Phys. Chem. Lett.* **7**(13), 2597–2601 (2016).
- 35 C. Dutta and A. V. Benderskii, *J. Phys. Chem. Lett.* **8**(4), 801–804 (2017).
- 36 M. Vinaykin and A. V. Benderskii, *J. Phys. Chem. Lett.* **3**(22), 3348–3352 (2012).
- 37 Y. Nagata, C.-S. Hsieh, T. Hasegawa, J. Voll, E. H. G. Backus, and M. Bonn, *J. Phys. Chem. Lett.* **4**(11), 1872–1877 (2013).
- 38 Y. Ni and J. Skinner, *J. Chem. Phys.* **143**(1), 014502 (2015).
- 39 D. R. Moberg, S. C. Straight, and F. Paesani, *J. Chem. Phys. B* **122**(15), 4356–4365 (2018).
- 40 T. Seki, S. Sun, K. Zhong, C.-C. Yu, K. Machel, L. B. Dreier, E. H. G. Backus, M. Bonn, and Y. Nagata, *J. Phys. Chem. Lett.* **10**, 6936 (2019).
- 41 M. Gouy, *J. Phys. Theor. Appl.* **9**(1), 457–468 (1910).
- 42 D. L. Chapman, *Philos. Mag.* **25**(148), 475–481 (1913).
- 43 J. A. Davis, R. O. James, and J. O. Leckie, *J. Colloid Interface Sci.* **63**(3), 480–499 (1978).
- 44 S.-H. Chen and S. J. Singer, *J. Chem. Phys. B* **123**, 6364 (2019).
- 45 M. A. Brown, Z. Abbas, A. Kleibert, R. G. Green, A. Goel, S. May, and T. M. Squires, *Phys. Rev. X* **6**(1), 011007 (2016).
- 46 G. Gonella, C. Lütgebaucks, A. G. De Beer, and S. Roke, *J. Phys. Chem. C* **120**(17), 9165–9173 (2016).
- 47 Y.-C. Wen, S. Zha, X. Liu, S. Yang, P. Guo, G. Shi, H. Fang, Y. R. Shen, and C. Tian, *Phys. Rev. Lett.* **116**(1), 016101 (2016).
- 48 T. Joutsuka and A. Morita, *J. Phys. Chem. C* **122**(21), 11407–11413 (2018).
- 49 S. Ong, X. Zhao, and K. B. Eisenthal, *Chem. Phys. Lett.* **191**(3–4), 327–335 (1992).
- 50 D. Gragson, B. McCarty, and G. Richmond, *J. Am. Chem. Soc.* **119**(26), 6144–6152 (1997).
- 51 A. M. Darlington, T. A. Jarisz, E. L. DeWalt-Kerian, S. Roy, S. Kim, M. S. Azam, D. K. Hore, and J. M. Gibbs, *J. Phys. Chem. C* **121**(37), 20229–20241 (2017).
- 52 K. C. Jena, P. A. Covert, and D. K. Hore, *J. Phys. Chem. Lett.* **2**(9), 1056–1061 (2011).

⁵³F. M. Geiger, *Annu. Rev. Phys. Chem.* **60**, 61–83 (2009).

⁵⁴P. E. Ohno, H.-f. Wang, and F. M. Geiger, *Nat. Commun.* **8**(1), 1032 (2017).

⁵⁵J. Schaefer, G. Gonella, M. Bonn, and E. H. G. Backus, *Phys. Chem. Chem. Phys.* **19**(25), 16875–16880 (2017).

⁵⁶M. D. Boamah, P. E. Ohno, E. Lozier, J. Van Ardenne, and F. M. Geiger, *J. Phys. Chem. B* **123**, 5848–5856 (2019).

⁵⁷S. Sun, R. Liang, X. Xu, H. Zhu, Y. R. Shen, and C. Tian, *J. Chem. Phys.* **144**(24), 244711 (2016).

⁵⁸X. Xu, Y. R. Shen, and C. Tian, *J. Chem. Phys.* **150**(14), 144701 (2019).